Postharvest Biology and Technology 183 (2022) 111739

Contents lists available at ScienceDirect

Postharvest Biology and Technology

journal homepage: www.elsevier.com/locate/postharvbio

Avocado dehydration negatively affects the performance of visible and near-infrared spectroscopy models for dry matter prediction

Puneet Mishra [a,*], Maxence Paillart [a], Lydia Meesters [a], Ernst Woltering [a,b], Aneesh Chauhan [a]

[a] Wageningen Food and Biobased Research, Bornse Weilanden 9, P.O. Box 17, 6700AA, Wageningen, the Netherlands
[b] Horticulture and Product Physiology Group, Wageningen University, Droevendaalsesteeg 1, P.O. Box 630, 6700AP, Wageningen, the Netherlands

ARTICLE INFO

Keywords:
Chemometrics
Multivariate
Fruit storage
Quality

ABSTRACT

This study aims to test the hypothesis that skin dehydration can cause the development of cork-like layers in the avocado fruit skin which may negatively affect Vis-NIR spectroscopy. To test this, dehydration treatment was applied on avocado fruit by storing them at low relative humidity (RH) during ripening treatment. Furthermore, to demonstrate that the hypothesis was not only valid for a single instrument and in general valid for any type of Vis-NIR instrument the avocados were also measured with two different spectrometers i.e., lab-based, and hand-held. Since the two instruments have two different measurement geometries i.e., diffuse reflection and interaction, the study also tests which geometry was best for the measurement of DMC in dehydrated avocados. The results showed that the dehydration of avocado fruit negatively affects the performance of Vis-NIR calibrations compared to the non-dehydrated fruit. The root mean squared error of cross-validation ($RMSE_{cv}$) on internal test set for dehydrated and non-dehydrated fruit were up to 1.49 % dw/fw and 1.02 % dw/fw, respectively. The hypothesis was true for both lab-based and hand-held instruments, and the root mean squared error of prediction on internal test set were up to 28 % higher for dehydrated fruits. The performance of interaction measurement mode was better ($RMSE_{cv}$ = 0.98 % dw/fw) than the diffuse reflection mode ($RMSE_{cv}$ = 1.21 % dw/fw) for non-dehydrated fruit, however, both modes achieved similar performance ($RMSE_{cv}$ = ~1.42 % dw/fw) for dehydrated fruit. The poorer performance of Vis-NIR models on dehydrated avocado fruit can be accepted as a limitation of Vis-NIR spectroscopy for avocado fruit analysis.

1. Introduction

Avocados are one of the most commercially important widely traded fruit across the world (Rodríguez-López et al., 2017). The avocado maturity stage is a key quality indicator that helps in decision making at several stages of the avocado supply chain such as during the harvest, grading of fruits during the packaging and during the storage at warehouses to facilitate year-round fruit availability (Li et al., 2018; Subedi and Walsh, 2020). A major indicator of avocado fruit maturity is the oil content (Ozdemir and Topuz, 2004; Rodríguez-López et al., 2017). However, measurement of oil content requires complex wet chemistry analysis which, from a time and cost perspective, is not an optimal solution (Clark et al., 2003). Studies have found that avocado oil content has a high correlation with the dry matter content (DMC) of the fruit (Clark et al., 2003). Since DMC measurement is easier (weighing – drying – weighing) and lower in cost compared to the oil content analysis, it is now widely used to assess the avocado maturity during various stages of the supply chain (Wedding et al., 2013). Nowadays even different non-destructive techniques are explored to predict the DMC in real-time to support rapid decision making (Li et al., 2018; Subedi and Walsh, 2020).

Visible and near-infrared spectroscopy (Vis-NIR) is one of the techniques for rapid non-destructive estimation of dry matter content (DMC) in fresh fruit (Subedi and Walsh, 2020). Application of Vis-NIR spectroscopy can be found ranging from assessment of small semi-transparent blueberries (Zheng et al., 2020) to big thick skin melons (Flores et al., 2008). Furthermore, applications range from the use of traditional lab-based benchtop instruments (Kasim et al., 2021) to portable handheld or pocket spectrometers (Mishra et al., 2021; Mishra and Woltering, 2021). For avocados as well, several applications to predict DMC using portable spectrometers can be found in the literature (Li et al., 2018; Subedi and Walsh, 2020). The Vis-NIR spectroscopy can predict the DMC because it captures the overtones of functional chemical bonds vibrations such as for OH, CH and NH bonds (Nicolai et al.,

* Corresponding author.
E-mail address: puneet.mishra@wur.nl (P. Mishra).

https://doi.org/10.1016/j.postharvbio.2021.111739
Received 16 July 2021; Received in revised form 15 September 2021; Accepted 16 September 2021
Available online 20 September 2021

2007). The main interesting overtone for DMC prediction is the OH (Subedi and Walsh, 2020). NIR signal related to the OH overtones can be directly correlated to the moisture in the fruit (Nicolai et al., 2007). Furthermore, since moisture is inversely related to the DMC, an inverse relationship exists between the NIR absorbance related to the OH overtone and the DMC in the fruit (Li et al., 2018; Subedi and Walsh, 2020). Such an inverse relation is modelled using chemometric regression techniques such as partial least-square (PLS) regression (Mishra et al., 2020; Saeys et al., 2019).

The Vis-NIR spectroscopy on fresh fruit is usually performed through the skin in either diffuse reflection or interaction mode (Walsh et al., 2020). In some cases, the transmission is preformed but that is limited to transparent or semi-transparent fruit (Nicolai et al., 2007; Walsh et al., 2020). The measurements through the skin, instead of directly on the fruit flesh, are done to avoid any damage to the fruit and to enable online sorting based on e.g., DMC. Previous experiments have shown that NIR light can penetrate the fruit skin by up to ~3−4 mm (Lammertyn et al., 2000; Nicolai et al., 2007). By penetrating inside, the NIR light can capture the properties of the fruit flesh (Walsh et al., 2020). Light penetration depends on the type of fruit. For a transparent or semi-transparent fruit like blueberry, light penetration can be remarkably high, while for some fruit with very thick skin like melon this could be exceptionally low. In the case of avocados, the light penetration is sufficient to be able to accurately predict the DMC in the fruit flesh as demonstrated in several applications (Li et al., 2018; Subedi and Walsh, 2020). However, in literature, most of the studies involved analysis of mature but unripe avocados (Li et al., 2018; Subedi and Walsh, 2020), where the skin and fruit flesh are well hydrated and connected to each other. 'Mature but unripe' avocados are harvested at mature stadium on the tree but unripe (not soft enough to be eaten).

During ripening, the tissue structure of the lower cell layers of the peel alters in such a way that the peel loses progressively its adhesion with the avocado flesh. (Espinosa-Velázquez et al., 2016) also reported that lignified thick walls in the lower cell layers and an increase in anthocyanin content. Cork-like tissue formation has also been reported in skin areas just under stomata or lenticels (Schroeder, 1950). The higher moisture loss may induce an early development of cork tissue in these areas. By consequence strong dehydration of the fruit during ripening process may enhance the formation of cork-like epidermis tissue. The cork-like tissue and the presence of air voids between the fruit flesh and skin may damp the NIR penetration, and therefore, diffuse reflection or interaction may bring back less information from the fruit flesh compared to the case when epidermis cells remain healthy. Such less information in the reflected NIR signals can lead to a poor estimation of the flesh properties when compared to the case where the exocarp remains tightly attached to mesocarp tissue (flesh tissue. To the best of our knowledge, no studies yet reported the effect of avocado skin dehydration on the performance of NIR models, and therefore, this work is the first to explore it.

This study has four main objectives; the first objective was to test the hypothesis that Vis-NIR calibration for DMC prediction performs poorly when the avocado fruit skin is dehydrated compared to a non-dehydrated fruit skin. The second objective was to test the hypothesis that such a poor model performance was independent of the instrument (lab-based or hand-held). The third objective was to test that irrespective of the measurement geometries (diffuse reflection or interaction) the DMC calibrations perform poorer for dehydrated fruit. Finally, as a fourth objective, global models for DMC prediction in avocado fruit were compared.

2. Materials and methods

2.1. Avocado fruit and storage treatment

580 avocados from South Africa (cultivar HASS, size 22, harvested in April 2020) were purchased from a Dutch importer. At reception, the avocados were stored at 5 °C and 85 % relative humidity (RH) at the post-harvest research facilities of Wageningen University & Research, The Netherlands for 2 days. 580 fruit were randomly distributed to 6 batches of 80 fruit each. Half of the fruits i.e., 240 (3 batches) were stored at a RH of 45 % to induce the skin dehydration, while the other half i.e., 240 (3 batches) were stored at an RH of 90 %. 90 % RH provides an ideal environment to prevent water loss and structural changes in the peel (Blakey, 2011; Erickson and Kikuta, 1964). For both the RH levels, temperature was maintained at 20 °C. Overall, the samples were measured during a period of 6 days and avocados were analysed on 2nd, 4th, and 6th days to cover a broad variation in fruit dehydration.

2.2. Spectral measurements

Two spectrometers were used for recording the visible and near-infrared spectra of avocado. The lab-based spectrometer was the lab-based Hi-Res LabSpec spectrometer (Analytical Spectral Devices, Malvern Panalytical, United Kingdom) and the hand-held spectrometer was a Felix F-750 (Felix Instruments, Camas, WA, USA). Both spectrometers were used at the exact same spot on the avocado fruit i.e., fruit belly. The measurements with lab-based spectrometer were performed prior to the hand-held instrument. There was no rationale in using the lab-based spectrometer before hand-held instrument, it was based on the availability of the operator during experiment. Both instruments have similar sized optical window i.e., ~20 mm diameter.

The lab-based spectrometer measures in the diffuse reflectance mode and in the spectral range of 350−2500 nm with 3 nm spectral sampling interval. The measurements were performed using the area scan probe (Hi-Brite probe) on the same positions where the reference measurements were done. The probe has an inbuilt 6.5 W halogen light source for illumination and the optical fibers to capture the reflected light. The instrument was controlled using the Indico Pro software (Analytical Spectral Devices, Malvern Panalytical, United Kingdom). The integration time was automatically optimized by the Indico Pro software and was defined as 15 milliseconds. 5 consecutive measurements (at the same spot) were averaged automatically by the Indico Pro software. The white reference used was a Spectralon white standard. The hand-held spectrometer measures spectra in the interaction mode covering the spectral range of 310−1135 nm with a ~3 nm spectral sampling interval. The hand-held spectrometer utilizes a Xenon Tungsten Lamp for illumination and a built-in white painted reference standard for estimating the reflectance.

For both the lab-base and hand-held spectrometer, the radiometric calibration with white and dark reference was performed as per Eq 1.

$$Reflectance = \frac{S - D}{W - D} \quad (1)$$

where, S is fruit spectra, D is dark reference spectra and W is white reference spectra.

2.3. Weight loss and reference dry matter measurements

The weight (g) of individual fruit was assessed on each evaluation day, including day 0, with the weighing balance (0-digit) incorporated in the AWETA acoustic firmness analyser (AWETA, The Netherlands). Weight loss was calculated by comparing the weight recording on evaluation day with weight measured on first experiment day. Weight loss was expressed in percentage (%) of the initial weight. After weight loss measurements, the skin and flesh tissue samples were collected with a cork borer of 1.6 cm diameter. Skin and flesh tissue were carefully separated from each other with a sharp knife. Tissues were placed into clean aluminium cups and initial weights (g) were recorded with a 3-digit analytical balance (Mettler-Toledo GmbH, Giessen, Germany). Later, the samples were dried in a hot-air oven (FD 56, Binder GmbH, Tuttlingen, Germany) at 80 °C for 60 h and the final weights (g) of the

aluminium cups were recorded with a 3-digit analytical balance (Mettler-Toledo GmbH, Giessen, Germany). DMC of skin and flesh was expressed in percent dry weight/fresh weight (% dw/fw).

2.4. Data analysis

2.4.1. Data pre-processing and partitioning

The spectra were obtained as reflectance and may contain global differences due to additive and multiplicative light scattering effects. Therefore, prior to any data modelling, the spectra were normalized for global differences in intensities by estimating the standard normal variate (SNV) (Barnes et al. 1989). Furthermore, Savitzky-Golay (Savitzky and Golay, 1964) 2nd derivative was used for unrevealing the underlying peaks on the SNV corrected data (Roger et al. 2020). Since in this study the samples were from two different RH levels, separate as well as global models to predict DMC in avocados were explored. For separate RH models, the spectra corresponding to each dehydration level were partitioned into calibration (70 %) and independent test (30 %) set using the Kennard-Stone (KS) algorithm (Kennard and Stone 1969).

2.4.2. Local and global partial least-squares regression modelling

Since this study involved comparing the performance of spectral models for different RH levels i.e., 45 % and 90 %, hence as a first comparison, individual partial least-squares (PLS) regression (Wold, 1987; Wold et al., 2001) models were established by optimising the latent variables (LVs) using a 5-fold Venetian blind cross-validation. The models were calibrated and tested on the data partitioned with the KS algorithm independently for each RH levels. As a second step of comparison, global models were established where the calibration set from each RH level were combined (obtained with the KS partitioning) and a new PLS regression model was computed by optimising the latent variables (LVs) using a 5-fold Venetian blind cross-validation. Later, the global model was tested on test data from each RH level independently. In this study, two different instruments operating in different spectral ranges were used i.e., lab-based (350−2500 nm) and the hand-held (310−1135 nm), and separate models for each instrument were developed. The lab-based spectrometer data was used in the complete spectral range (350−2500 nm), whereas, for the hand-held spectrometer the spectral range was reduced to 400−999 nm due to the presence of noise in the extreme wavelengths. Since the lab-based instrument has a broader spectral range, to have a fair comparison with the hand-held instrument, models based on the reduced spectral range (400-999 nm) of the lab-based instrument were also explored. One extra global model for the hand-held instrument was explored based on the NIR spectral range (720−999 nm) of data to avoid any influence of the outer skin colour (Subedi and Walsh, 2020). Therefore, in total, four types of models were explored:

- model based on 350−2500 nm spectral data from the lab-based instrument
- model based on 400−999 nm spectral data from lab-based instrument
- model based on 400−999 nm spectral data from the hand-held instrument
- global model (based on data from both dehydrated and non-dehydrated fruit) based on 720−999 nm spectral data from hand-held instrument.

All model performances were presented as the root mean squared error of cross-validation on internal test set ($RMSE_{cv}$ % dw/fw), standard error of cross-validation on internal test set (SE_{cv} % dw/fw) and bias (% dw/fw). A key point to note that in this study the test set was made up of data from the same experimental design and will be denoted as the internal test set in the following part of manuscript, also the cross-validation parameters are the performance of model on the internal test set. All analysis were performed in MATLAB 2018b (Natick, MA, USA).

3. Results and discussion

3.1. Dehydration visual symptoms

The ripening of avocado fruit led to detachment of fruit skin from the flesh. Loss of adhesion between the hypodermis cell layer and the mesocarp tissue occurs when fruit soften and get ‘Ready to Eat’. When fruit is healthy and the ripening process is applied with 90 % RH, hypodermis cells remain hydrated (light green colour on Fig. 1A). At the contrary, when lenticels are damaged (Fig. 1B) or when strong dehydration occurs during ripening (ripening at 45 % RH) (Fig. 1C), the hypodermis cells develop into cork-like tissue and dehydrate completely. In this study, it has been hypothesized that the presence of the cork-like tissue (Fig. 1B, C) developed during the fruit dehydration can act as a barrier to the penetration of Vis-NIR light, hence, effecting the net analyte signal captured by the reflected/interacted spectra. Vis-NIR light, hence, effecting the net analyte signal captured by the reflected/interacted spectra.

3.2. Spectra and reference dry matter measurements

The mean pre-processed spectra in the spectral range of 350−2500 nm for avocados stored at 45 % (black thick line) and 90 % RH (red thin line) levels at 6th measurement day are shown in Fig. 2A. The spectral data for the 6th measurement day are shown as it was the last day of treatment and assumed to have the highest contrast between hydrated and dehydrated fruit skin. The specta for avocados stored at different RH levels have peaks at similar wavelengths, however, their are underlying differences in intensities which are difficult to note in Fig. 2A. To gain insight to the difference between mean spectra of avocados from different RH levels, the mean difference spectra is shown in Fig. 2B. In the mean difference spectra, the key difference can be noted over several spectral wavelengths. The main difference can be noted related to the degradation of colour between 500−600 nm, red-edge region 670−720 nm, 1st (1950 nm), 2nd (1400 nm), 3rd overtones of H_2O (750 and 960 nm), and 2nd overtones (1150 nm) related to CH bonds (Osborne et al., 1993). Physiologically, the difference in the colour and the red-edge region can be related to the degradation of avocado skin pigment i.e. chlorophyll and the decrease in the phytosynthetic activity, respectively. The differences in the several H_2O overtones can be related to the fruit dehydration and moisture loss. The difference related to the CH bond could be related to the change in the sugar forms as commonly in the case of avocados the C_7 sugar is consumed and leaving behind only the C_6 sugars (Osborne et al., 1993).

Fig. 3 shows different reference measurements performed on each avocado fruit. The histogram for DMC measured on fruit flesh and skin are shown in Fig. 3A, B, respectively. At a first glance, it can be noted that the DMC of the skin was higher than the DMC of flesh, which is directly in accordance with the DMC values reported in earlier studies (Subedi and Walsh, 2020). The DMC of fruit flesh and skin for avocados stored at different RH showed similar distribution, indicating a small effect of dehydration on the DMC of flesh and skin. The calculated DMC was determined by the loss of water from the fruit as the loss of carbon through respiration was expected to be very minor. There was a distinct pattern in the weight loss for avocado stored at RH 45 % (Fig. 3C). The dehydration by storing avocado at 45 % RH caused up to 12 % weight loss compared to a maximum of 6 % weight loss in the fruit stored at 90 % RH. Such a high weight loss by storing at a low RH level confirms that the fruit stored at 45 % RH suffered dehydration as expected by the treatment. Although in the histogram plot (Fig. 3) it was unclear how the DMC of skin and flesh changed along the observation during 3 different measurement days. To explain that better the *mean* ± *std* values for DMC of skin and flesh are shown in Table 1. The main point to note (Table 1)

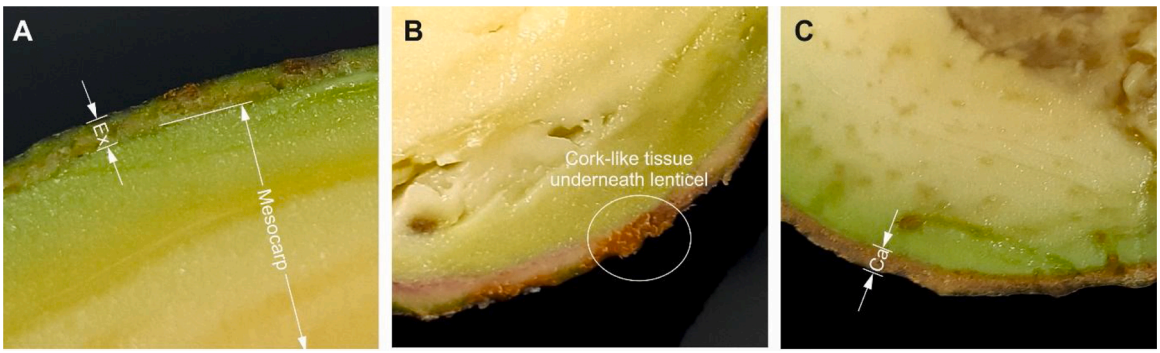

Fig. 1. Cross section of ready to eat avocado with different dehydration symptoms. Avocado ripened under 90 % relative humidity (A) with light green exocarp tissue (Ex). Cork-like tissue (Ca) produced in the hypodermis cell layer just under lenticel area (B) or when avocado has ripened at low relative humidity (C) For interpretation of the references to colour in this figure legend, the reader is referred to the web version of this article.).

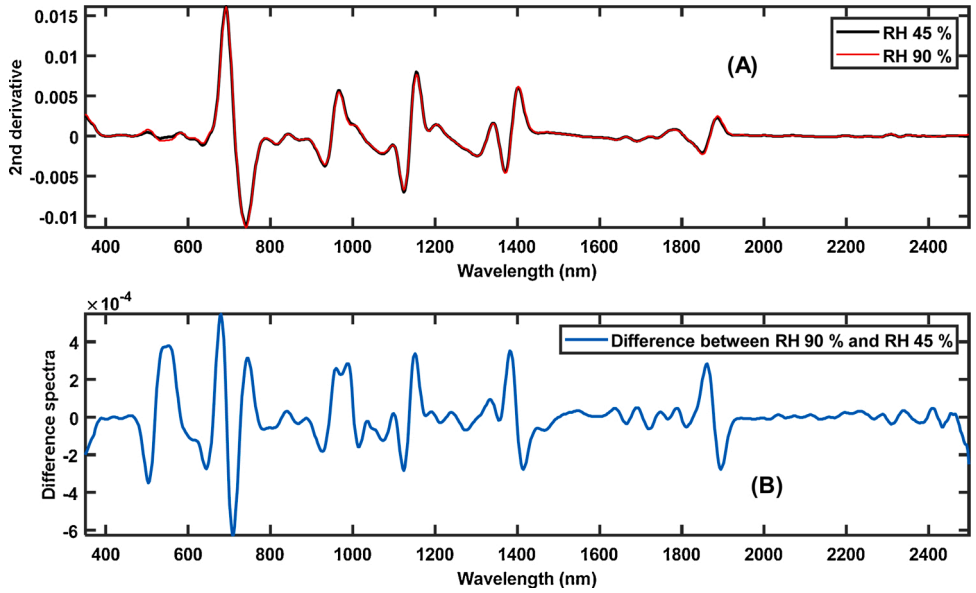

Fig. 2. (A) Mean 2nd derivative spectra of avocado fruit (350-2500 nm) stored at two different relative humidity (RH) levels i.e., 45 % (black thick line) and 90 % (red thin line) during the last observation day. (B) Mean difference between the spectra of avocado fruit stored at two different RH levels i.e., 45 % and 90 % (For interpretation of the references to colour in this figure legend, the reader is referred to the web version of this article.).

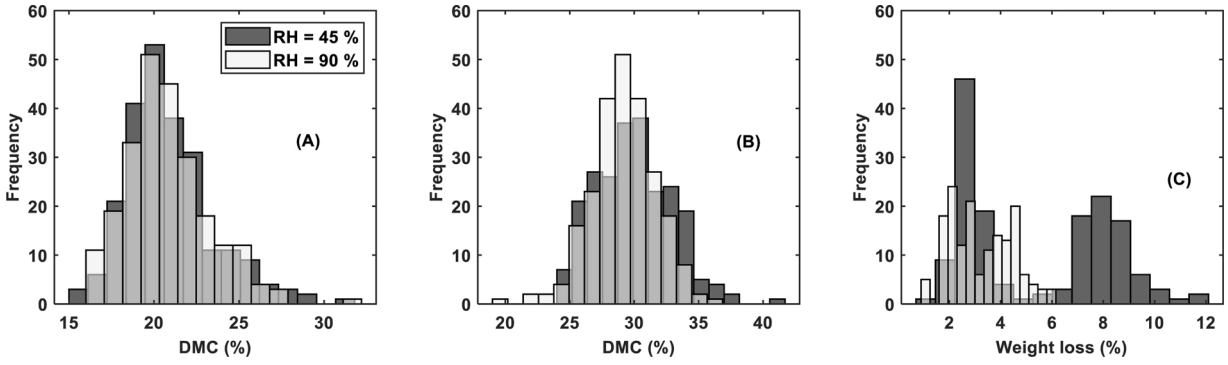

Fig. 3. Histograms for dry matter content (DMC % dw/fw) and weight loss (%) for fruits at different RH levels i.e., 45 % (red) and 90 % (Grey). (A) DMC of fruit flesh, (B) DMC of fruit skin, and (C) weight loss (%) of fruit.

was that the DMC of flesh under different RH storages did not change while the DMC of skin was remarkably increased indicating the clear effect of skin dehydration due to fruit storage at different RH levels.

3.3. Partial least-square regression models

To this point, it has been demonstrated that the avocado fruit stored at 45 % RH suffered from dehydration and the effect of dehydration can be noted at several spectral wavelengths (Fig. 2B). The next step was to

Table 1
A summary of dry matter content (DMC % dw/fw) of skin and flesh at different experiment day under different relative humidity levels.

Properties	45 % relative humidity			90 % relative humidity		
	2^{nd} day (mean ± std)	4^{th} day (mean ± std)	6^{th} day (mean ± std)	2^{nd} day (mean ± std)	4^{th} day (mean ± std)	6^{th} day (mean ± std)
DMC flesh	20.47 ± 2.22	21.49 ± 2.64	21.10 ± 3.20	21.25 ± 2.56	20.61 ± 2.64	20.34 ± 2.52
DMC skin	28.57 ± 2.26	29.78 ± 2.46	32.43 ± 4.55	29.28 ± 2.72	29.15 ± 2.52	29.23 ± 2.10

explore the performance of Vis-NIR models for DMC prediction of fruit stored at different RH levels. Hence, the performance of PLS models calibrated and tested independently for different RH levels are shown in Fig. 4. The left column is for the dehydrated samples and the right column is for the non-dehydrated samples. The performance of the models for dehydrated samples was poorer compared to the non-dehydrated samples. Furthermore, it was valid for both the lab based as well as the hand-held instrument. The performance of the hand-held instrument that measured samples in the interaction geometry was better than the lab-based instrument measuring samples in the diffuse reflectance. Furthermore, the performance of the hand-held instrument (interaction) was far better than the lab-based instrument (diffuse reflection) for non-dehydrated samples compared to the dehydrated samples.

In DMC modelling with Vis-NIR spectroscopy, a poor focus is paid to the dehydration level of avocados. Usually, the models are measured on non-dehydrated avocados. However, such a model made on non-dehydrated fruit may perform poorly when tested on dehydrated fruit due to a global difference in the hydration level of fruit. The results of

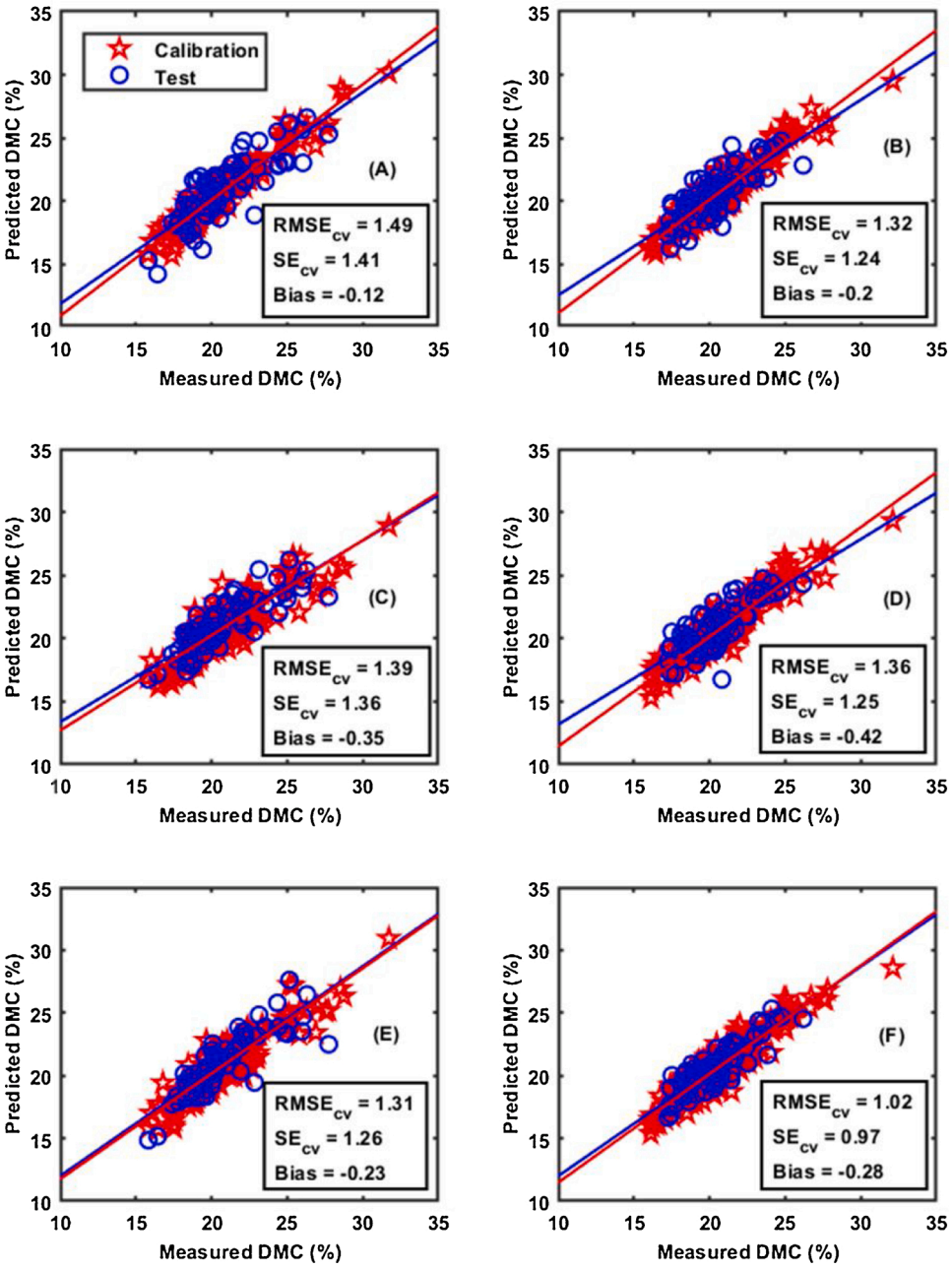

Fig. 4. Partial least-square (PLS) calibrations to predict dry matter content (DMC % dw/fw) in avocado flesh for fruit stored at different relative humidity (RH) levels i.e., 45 % (left column) and 90 % (right column). PLS calibration with Labspec 400-2500 nm spectral data for RH (A) 45 %, and (B) 90 %. PLS calibration with Labspec 400-1000 nm spectral data for RH (C) 45 %, and (D) 90 %. PLS calibration with Felix 400-1000 nm spectral data for RH (E) 45 %, and (F) 90 %. The calibration set are presented in red stars and independent test set in blue circles. Root mean squared error of cross-validation on internal test set ($RMSE_{cv}$), standard error of cross-validation on internal test set (SE_{cv}), and Bias are in % dw/fw (For interpretation of the references to colour in this figure legend, the reader is referred to the web version of this article.).

testing the model made on non-dehydrated fruit (left column) tested on dehydrated fruit (right column) are shown in Fig. 5. The model made on non-dehydrated fruit (Fig. 5, left column) indeed, poorly when tested on the dehydrated fruit (Fig. 5, right column), as the $RMSE_{cv}$'s were increased drastically. Furthermore, the inferior performance was noted for both lab-based (diffused reflection) and hand-held (interaction) instrument.

3.4. Performance of global models

In the presence of both dehydrated and non-dehydrated samples (e.g., a partly ripened batch), one could expect that a better solution could be to develop a global model which covers the wide variation between the dehydrated and non-dehydrated samples. Hence, the performance of global models for non-dehydrated (left column) and dehydrated (right column) samples are shown in Fig. 6. Compared to performance of the model made independently for dehydrated and non-dehydrated fruit (Fig. 4), the global models showed much lower $RMSE_{cv}$ for both the non-dehydrated and dehydrated fruit, indicating a clear benefit of global modelling. The improvement was noted for both non-dehydrated as well as dehydrated samples and for both hand-held (interaction) and lab-based (diffuse reflection) instruments. However, even after the global modelling, the $RMSE_{cv}$ for dehydrated samples was much higher compared to the non-dehydrated samples. For example, the $RMSE_{cv}$ of the global model based on hand-held instrument data for non-dehydrated samples was 0.98 % dw/fw, while for dehydrated samples the $RMSE_{cv}$ was 1.36 % dw/fw. Such an inferior performance of global models for dehydrated fruits confirms that fruit dehydration negatively effects the performance of Vis-NIR calibration models.

For the hand-held instrument, an extra global model was explored in the NIR spectral range of 720−999 nm. The reason was because in that spectral range the overtones related to H_2O were present and hence a good correlation with the DMC in fresh fruit can be achieved. Also, by restricting the model to the NIR spectral range the model can be more

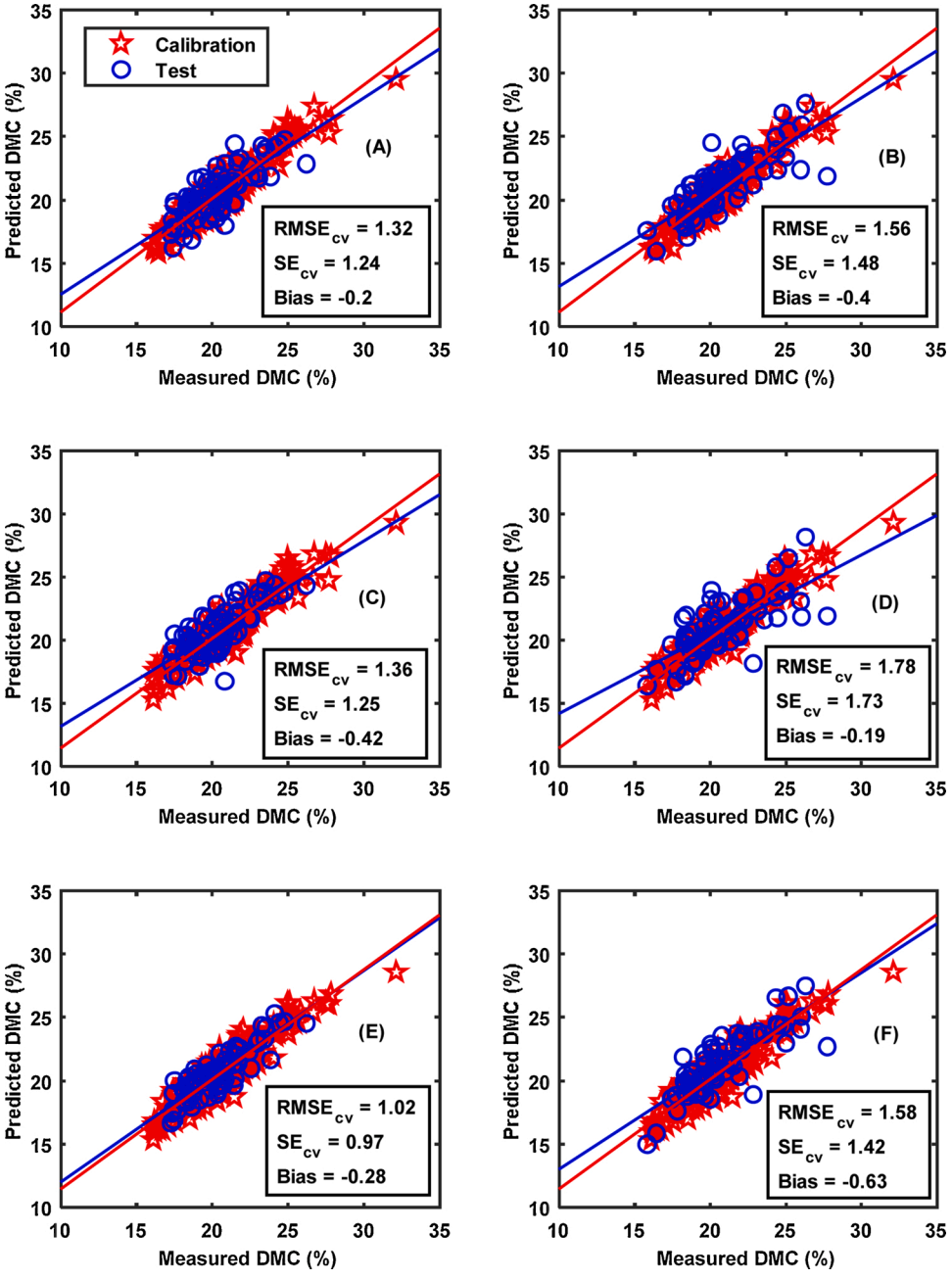

Fig. 5. Partial least-square (PLS) calibrations made on data from relative humidity (RH) 90 % (left column) tested on data from RH 45 % (right column) to predict dry matter content (DMC % dw/fw). PLS calibration with Labspec 400-2500 nm spectral data for RH (A) 90 %, and (B) tested on RH 45 % data. PLS calibration with Labspec 400-1000 nm spectral data for RH (C) 90 %, and (D) tested on RH 45 % data. PLS calibration with Felix 400-1000 nm spectral data for RH (E) 90 %, and (F) tested on RH 45 % data. The calibration set are presented in red stars and independent test set in blue circles. Root mean squared error of cross-validation on internal test set ($RMSE_{cv}$), standard error of cross-validation on internal test set (SE_{cv}), and Bias are in % dw/fw (For interpretation of the references to colour in this figure legend, the reader is referred to the web version of this article.).

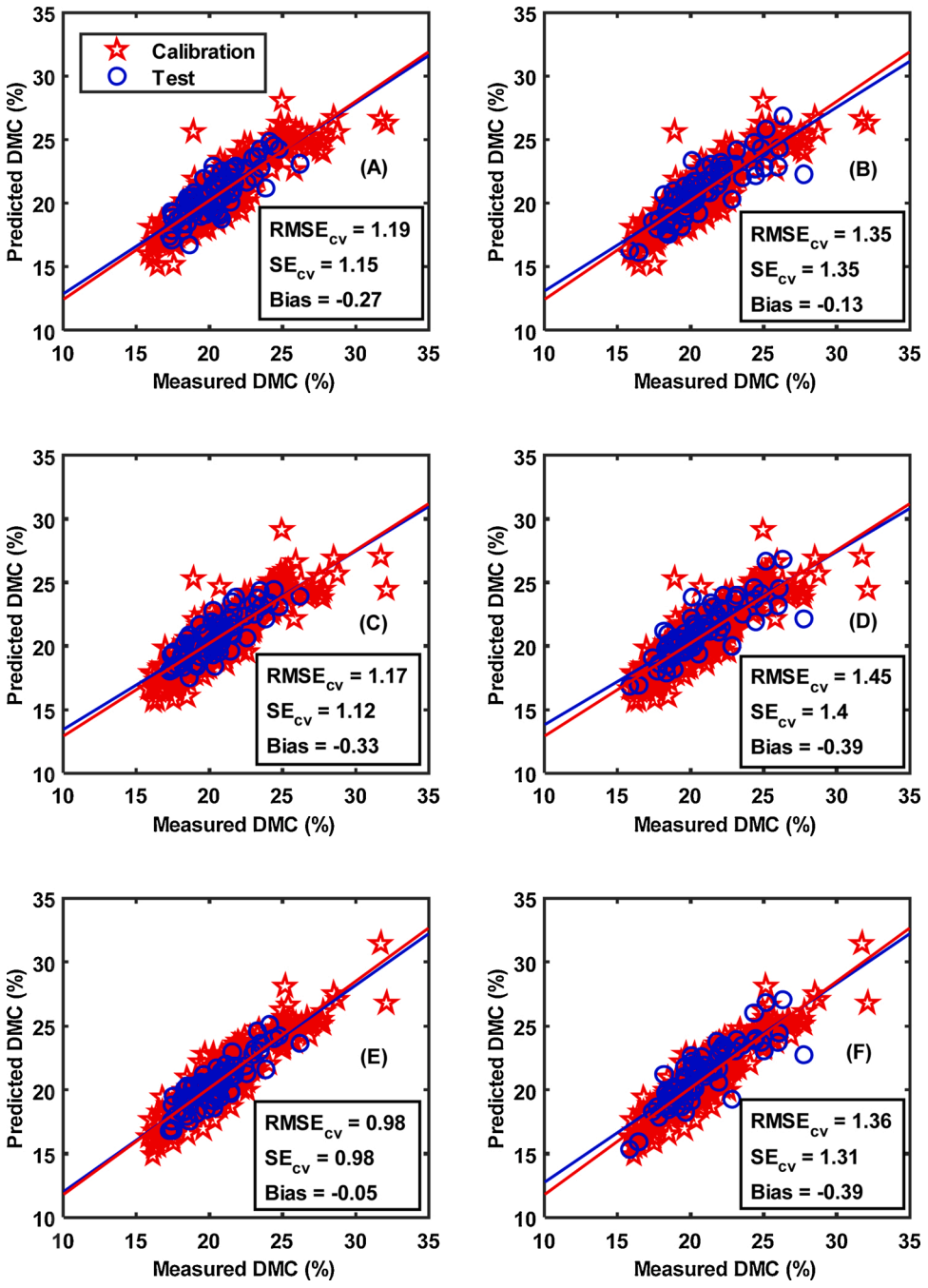

Fig. 6. Performance of global partial least-square model tested on data from 90 % relative humidity (RH) (left column) and 45 % RH (right column) to predict dry mater content (DMC % dw/fw). Updated PLS calibration with Labspec 400-2500 nm spectral data for RH (A) 90 %, and (B) tested on RH 45 % data. Updated PLS calibration with Labspec 400-1000 nm spectral data for RH (C) 90 %, and (D) tested on RH 45 % data. Updated PLS calibration with Felix 400-1000 nm spectral data for RH (E) 90 %, and (F) tested on RH 45 % data. The calibration set are presented in red stars and independent test set in blue circles. Root mean squared error of cross-validation on internal test set ($RMSE_{cv}$), standard error of cross-validation on internal test set (SE_{cv}), and Bias are in % dw/fw (For interpretation of the references to colour in this figure legend, the reader is referred to the web version of this article.).

robust to the change in the outer peel colour of the fruit. Hence, based on the recommendation of the hand-held instrument manufacturer, the global models were also explored for only the NIR spectral range (720−999 nm) of the hand-held instrument. The performances of global models based on NIR spectral range are shown in Fig. 7. Like the performance of the global model based on the complete spectral range (400−1000 nm), the performance of global models based on NIR spectral range was better for non-dehydrated (Fig. 7-A) samples compared to the dehydrated (Fig. 7B) samples. Furthermore, the performance of model based on NIR spectral range was poorer compared to the complete spectral range (400−1000 nm). For example, the $RMSE_{cv}$ of the non-dehydrated samples based on the complete spectral range (400−1000 nm) was 0.98 % dw/fw, while for the NIR spectral range was 1.02 % dw/fw. Although such a small difference cannot be considered as a significant difference considering the high uncertainty with the spectral measurements and the reference analysis.

4. Discussion

In scientific literature, Vis-NIR spectroscopy has been widely explored for DMC prediction in avocado ('Hass') fruit and a wide variation in the accuracy of Vis-NIR is reported. For example, NIR analysis of intact fruit ('Hass') attained RMSEP = 1.8 % (Clark et al., 2003), NIR analysis on avocados ('Hass') ripened after water and ABA infusion attained SEP = 1.8 % (Blakey et al., 2009), NIR model developed based on data ('Hass') from 3 consecutive years of harvest attained RMSEP = 1.43 % (Wedding et al., 2013), a global model combining data from three different cultivars i.e., 'Fuerte', 'Hass', and 'Carmen', attained $RMSE_{cv}$ = 2.94 % (Blakey, 2016), and NIR analysis performed for avocado ('Sepherd' and 'Hass') with skin and without skin attained

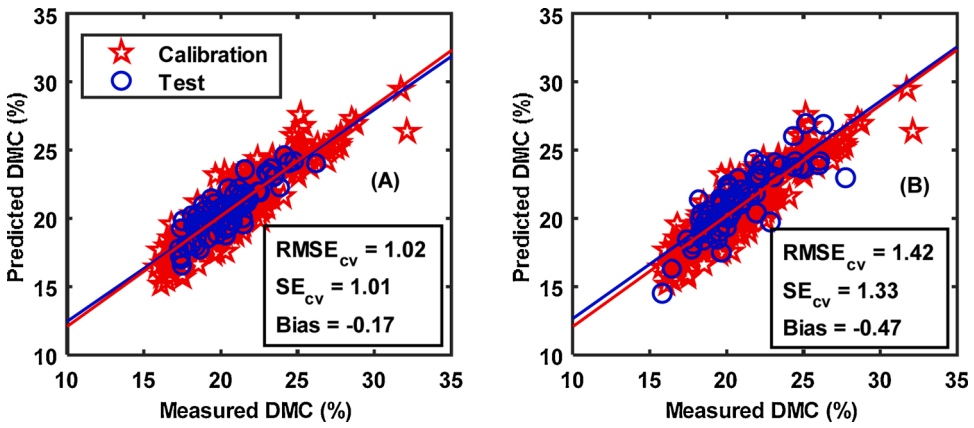

Fig. 7. The performance of global models calibrated in spectral range of 720-999 nm for Felix instrument and tested on fruit samples from different relative humidity (RH) to predict dry matter content (DMC % dw/fw) (A) 90 %, and (B) 45 %. Root mean squared error of cross-validation on internal test set (RMSE$_{cv}$), standard error of cross-validation on internal test set (SE$_{cv}$), and Bias are in % dw/fw.

RMSE$_{cv}$ of 1.38 % for intact 1.21 %, respectively (Subedi and Walsh, 2020). Compared to earlier studies, the accuracy attained in this study were better for non-dehydrated fruit (RMSE$_{cv}$ = 1.02 %) or comparable for dehydrated fruit (RMSE$_{cv}$ = 1.42 %). The model accuracy attained in this study for 'Hass' avocado was slightly poorer than attained earlier for 'Ettinger' variety RMSEP = 0.9 % (Schmilovitch et al., 2001). However, a reason for better performance of NIR models on 'Ettinger' variety could be related to the smooth texture thin skin, while 'Hass' has a thick texture skin, less conducive to light transmission (Clark et al., 2003). The thickness of fruit skin can directly influence the NIR analysis for DMC measurements as during NIR analysis the light is passed through the skin and interact with the mesocarp of the fruit and later while coming back to the detector must pass through the skin once again (Subedi and Walsh, 2020). Furthermore, there are already evidences that the skin in avocados causes a detrimental effect on the performance of DMC models for avocados, for example, the lower RMSE$_{cv}$ attained in an earlier study for NIR analysis performed on skin removed fruit compared to the high RMSE$_{cv}$ for NIR analysis performed on fruit with skin, suggest that the contribution of the skin to the NIR models is large (Subedi and Walsh, 2020).

In this study, it was noted that the interaction mode achieved lower RMSE$_{cv}$ for non-dehydrated fruit compared to the diffuse reflection mode. The results agreed with an earlier study where a comparison of interaction and reflection mode showed the superiority of interaction mode in predicting DMC in avocado fruit (Clark et al., 2003).

The main hypothesis of this study that fruit dehydration brings alteration in the skin structure which further influences the performance of the NIR model was found to be true as the NIR models developed on fruit with dehydrated skin showed higher RMSE$_{cv}$ compared to non-dehydrated fruit. This agreed with the hypothesis proposed in a recent study (Subedi and Walsh, 2020) where it was hypothesized that changes in the skin characteristics may deteriorate the NIR models by contributing to extra bias. However, in an earlier study, it was concluded that the higher bias was due to changes in the fruit flesh and not due to the skin (Subedi and Walsh, 2020). Although the hypothesis proposed in this study and the one proposed in (Subedi and Walsh, 2020) appears similar, however, the underlying experiments were different. In this study, we provided artificial dehydration to the fruit and confirmed the changes in the skin properties that can influence the NIR models, while in the earlier study (Subedi and Walsh, 2020), there were no justifications if there were any alterations in the skin characteristics as the hypothesis was validated by performing NIR analysis on fruit flesh.

5. Conclusions

This study showed that dehydration of avocado fruit under storage in low RH conditions stimulated the production of cork-like cell tissue, which caused the detachment of the fruit skin from the flesh. Such change in skin tissue structure negatively affected the Vis-NIR spectroscopy of dehydrated fruit. The Vis-NIR calibration models related to DMC prediction suffered from the presence of cork-like tissue. This study showed that irrespective of the Vis-NIR instrument i.e., lab-based, or hand-held, spectral range and the measurement mode i.e., diffuse reflection or interaction, the performance of Vis-NIR models for predicting DMC performed poorer for dehydrated fruit compared to non-dehydrated fruit. The performance of interaction measurement mode was better than the diffuse reflection mode for non-dehydrated fruit, however, both modes achieved similar performance for dehydrated fruit. Such an inferior performance of Vis-NIR models for DMC prediction on dehydrated avocado fruit is the limitation of Vis-NIR spectroscopy. Currently, it is unclear how an accurate non-destructive estimation of DMC of dehydrated avocados can be performed, a solution could be to develop a multi-sensor framework; however, this will be the topic for future research.

CRediT authorship contribution statement

Puneet Mishra: Conceptualization, Methodology, Software, Formal analysis, Writing - original draft. **Maxence Paillart:** Conceptualization, Methodology, Writing - original draft. **Lydia Meesters:** Conceptualization, Methodology, Writing - original draft, Supervision, Project administration. **Ernst Woltering:** Writing - review & editing, Supervision. **Aneesh Chauhan:** Writing - review & editing, Project administration, Funding acquisition.

Declaration of Competing Interest

The authors report no declarations of interest.

Acknowledgments

This work was financially supported by LNV (Dutch Ministry of Agriculture, Nature and Food Quality) funded Sensing Potential project (ref: KB-38-001-008) and by European Union's Horizon 2020 research and innovation programme under grant agreement No 739570, project ANTARES.

References

Blakey, R.J., 2011. Management of Avocado Postharvest Physiology. In PhD Thesis. https://doi.org/10.13140/RG.2.1.3652.7121.

Blakey, R.J., 2016. Evaluation of avocado fruit maturity with a portable near-infrared spectrometer. Postharvest Biol. Technol. 121, 101–105. https://doi.org/10.1016/j.postharvbio.2016.06.016.

Blakey, R.J., Bower, J.P., Bertling, I., 2009. Influence of water and ABA supply on the ripening pattern of avocado (Persea americana Mill.) fruit and the prediction of water content using Near Infrared Spectroscopy. Postharvest Biol. Technol. 53, 72–76. https://doi.org/10.1016/j.postharvbio.2009.03.004.

Clark, C.J., McGlone, V.A., Requejo, C., White, A., Woolf, A.B., 2003. Dry matter determination in 'Hass' avocado by NIR spectroscopy. Postharvest Biol. Technol. 29, 301–308. https://doi.org/10.1016/S0925-5214(03)00046-2.

Erickson, L.C., Kikuta, Y., 1964. Ripening Hass avocados in high and low humidities. Calif. Avoc. Soc. Yearb 48, 90–91 doi: N/A.

Espinosa-Velázquez, R., Dorantes-Álvarez, L., Gutiérrez-López, G.F., García-Armenta, E., Sánchez-Segura, L., Perea-Flores, M.J., Ceballos-Reyes, G.M., Ortíz-Moreno, A., 2016. Morpho-structural description of unripe and ripe avocado pericarp (Persea americana Mill var. drymifolia). Revista Mexicana de Ingeniería Química 15, 469–480. https://doi.org/10.24275/rmiq/Alim1144.

Flores, K., Sánchez, M.T., Pérez-Marín, D.C., López, M.D., Guerrero, J.E., Garrido-Varo, A., 2008. Prediction of total soluble solid content in intact and cut melons and watermelons using near infrared spectroscopy. J. Near Infrared Spectrosc. 16, 91–98. https://doi.org/10.1255/jnirs.771.

Kasim, N.F.M., Mishra, P., Schouten, R.E., Woltering, E.J., Boer, M.P., 2021. Assessing firmness in mango comparing broadband and miniature spectrophotometers. Infrared Phys. Technol. 115, 103733 https://doi.org/10.1016/j.infrared.2021.103733.

Lammertyn, J., Peirs, A., De Baerdemaeker, J., Nicolaï, B., 2000. Light penetration properties of NIR radiation in fruit with respect to non-destructive quality assessment. Postharvest Biol. Technol. 18, 121–132. https://doi.org/10.1016/S0925-5214(99)00071-X.

Li, M., Qian, Z.Q., Shi, B.W., Medlicott, J., East, A., 2018. Evaluating the performance of a consumer scale SCiO (TM) molecular sensor to predict quality of horticultural products. Postharvest Biol. Technol. 145, 183–192. https://doi.org/10.1016/j.postharvbio.2018.07.009.

Mishra, P., Woltering, E., 2021. Handling batch-to-batch variability in portable spectroscopy of fresh fruit with minimal parameter adjustment. Anal. Chim. Acta 1177, 338771. https://doi.org/10.1016/j.aca.2021.338771.

Mishra, P., Roger, J.M., Marini, F., Biancolillo, A., Rutledge, D.N., 2020. FRUITNIR-GUI: a graphical user interface for correcting external influences in multi-batch near infrared experiments related to fruit quality prediction. Postharvest Biol. Technol., 111414 https://doi.org/10.1016/j.postharvbio.2020.111414.

Mishra, P., Marini, F., Brouwer, B., Roger, J.M., Biancolillo, A., Woltering, E., Echtelt, E. H.-v., 2021. Sequential fusion of information from two portable spectrometers for improved prediction of moisture and soluble solids content in pear fruit. Talanta 223, 121733. https://doi.org/10.1016/j.talanta.2020.121733.

Nicolai, B.M., Beullens, K., Bobelyn, E., Peirs, A., Saeys, W., Theron, K.I., Lammertyn, J., 2007. Nondestructive measurement of fruit and vegetable quality by means of NIR spectroscopy: a review. Postharvest Biol. Technol. 46, 99–118. https://doi.org/10.1016/j.postharvbio.2007.06.024.

Osborne, B.G., Fearn, T., Hindle, P.H., 1993. Practical NIR spectroscopy with applications in food and beverage analysis. Longman scientific and technical. ISBN : 0-582-09946-3 doi: N/A.

Ozdemir, F., Topuz, A., 2004. Changes in dry matter, oil content and fatty acids composition of avocado during harvesting time and post-harvesting ripening period. Food Chem. 86, 79–83. https://doi.org/10.1016/j.foodchem.2003.08.012.

Rodríguez-López, C.E., Hernández-Brenes, C., Treviño, V., Díaz de la Garza, R.I., 2017. Avocado fruit maturation and ripening: dynamics of aliphatic acetogenins and lipidomic profiles from mesocarp, idioblasts and seed. BMC Plant Biol. 17 https://doi.org/10.1186/s12870-017-1103-6, 159-159.

Saeys, W., Do Trong, N.N., Van Beers, R., Nicolai, B.M., 2019. Multivariate calibration of spectroscopic sensors for postharvest quality evaluation: a review. Postharvest Biol. Technol. 158. https://doi.org/10.1016/j.postharvbio.2019.110981.

Savitzky, A., Golay, M.J.E., 1964. Smoothing and differentiation of data by simplified least squares procedures. Anal. Chem. 36, 1627–1639. https://doi.org/10.1021/ac60214a047.

Schmilovitch, Z., Hoffman, A., Egozi, H., El-Batzri, R., Degani, C., 2001. Determination of avocado maturity by near-infrared spectrometry. Acta Horticulturae. International Society for Horticultural Science (ISHS), Leuven, Belgium, pp. 175–179. https://doi.org/10.17660/ActaHortic.2001.562.19.

Schroeder, C.A., 1950. The Structure of the Skin or Rind of the Avocado, 34. California Avocado Society Yearbook, pp. 169–176 doi: N/A.

Subedi, P.P., Walsh, K.B., 2020. Assessment of avocado fruit dry matter content using portable near infrared spectroscopy: Method and instrumentation optimisation. Postharvest Biol. Technol. 161. https://doi.org/10.1016/j.postharvbio.2019.111078.

Walsh, K.B., Blasco, J., Zude-Sasse, M., Sun, X., 2020. Visible-NIR 'point' spectroscopy in postharvest fruit and vegetable assessment: the science behind three decades of commercial use. Postharvest Biol. Technol. 168, 111246. https://doi.org/10.1016/j.postharvbio.2020.111246.

Wedding, B.B., Wright, C., Grauf, S., White, R.D., Tilse, B., Gadek, P., 2013. Effects of seasonal variability on FT-NIR prediction of dry matter content for whole Hass avocado fruit. Postharvest Biol. Technol. 75, 9–16. https://doi.org/10.1016/j.postharvbio.2012.04.016.

Wold, S., 1987. PLS Modeling With Latent Variables in Two or More Dimensions. doi: N/A.

Wold, S., Sjostrom, M., Eriksson, L., 2001. PLS-regression: a basic tool of chemometrics. Chemom. Intell. Lab. Syst. 58, 109–130. https://doi.org/10.1016/S0169-7439(01)00155-1.

Zheng, W., Bai, Y., Luo, H., Li, Y., Yang, X., Zhang, B., 2020. Self-adaptive models for predicting soluble solid content of blueberries with biological variability by using near-infrared spectroscopy and chemometrics. Postharvest Biol. Technol. 169, 111286 https://doi.org/10.1016/j.postharvbio.2020.111286.